concretenz
BUILDING RESILIENCE
CONFERENCE 2022
13-15 October 2022
Energy Events Centre | Rotorua

MIX DESIGN AND FRESH PROPERTIES OF 3D PRINTED CONCRETE

GIUSEPPE LOPORCARO & DON CLUCAS

University of Canterbury

SUMMARY

Digital fabrication and additive manufacturing may revolutionize the construction industry due to their potential advantages such as faster construction, waste minimisation, less human labour, improved accuracy and on-site safety improvements. Moreover, concrete additive manufacturing has a unique advantage over typical concrete construction because of its ability to construct architectural and structural components without the use of formwork. Although additive manufacturing in construction has been researched for over a decade, little research is available in the New Zealand context.

3D printing consists of the deposition of successive layers of concrete which is generally pumped to a nozzle which size may vary from 9 to 30 mm, approximately. The nozzle may be attached to either a robotic arm, a frame or a gantry system and it is computer controlled. This type of construction method requires that the material meets requirements that are not usually required for ordinary in-situ casted concrete.

At the University of Canterbury, a medium-scale custom-made 3D printer for concrete has been designed and built. After an introduction to the design and construction of the 3D concrete printer, this paper discusses the development of three mix designs of 3D printable concrete and compare the experimental results concerning the fresh material properties of these mixes.

The mixes were evaluated based on extrudability (through a 10-mm nozzle), workability, open time and buildability. The mix designs that varied in ratios of locally sourced New Zealand materials (river sand, Portland cement, fly ash and silica fume) were compared based on the latter properties. The mixes also contained various quantities of super plasticiser and fibre reinforcements (no fibre, polyvinyl alcohol or polypropylene). The mixes containing fibres had the most desirable workability characteristics as the fibres improved the binding properties of the mix. The mix containing polypropylene fibres showed the lowest workability in the ASTM drop table test, which was consistent in further testing as it extruded a narrower and less consistent filament. The optimum mix was the mix containing PVA fibres with a 3:2 sand-binder and 0.27 water-cement ratio. This mix had optimal workability and extrudability characteristics and showed little deformation under the load of the subsequent layers.

INTRODUCTION

The use of concrete in construction dates back to the Roman Empire in the third century BC. Concrete (*opus caementicium*) for construction was made by mixing sandy volcanic ash and lime mortar such as that used in the Pantheon. Modern concrete, made of Portland cement and coarse aggregate, was produced from the beginning of the 1800s. The invention of reinforced concrete is often attributed to Joseph Monier, who patented the idea of combining concrete and round steel bars in flexural members in 1877. However, it is the French constructor François Hennebique who gave the biggest impulse to the spread of reinforced concrete in construction (Soderstrom, 2020). Statistics from Stats NZ show that the use of ready-mixed concrete was approximately 4 million cubic metres over the last five years (http://infoshare.stats.govt.nz/).

The success of reinforced concrete is due to multiple reasons such as its strength which allow obtaining slender structures able to span long distances, the resistance to fire and the ability to be moulded and shaped in different forms, providing flexibility in terms of material placement, handling and creative geometry. However, it typically involves formwork and steel reinforcement which requires considerable time and labour to set up and constrains building geometries.

New age construction has seen digital fabrication and additive manufacturing as promising avenues of construction due to its potential advantages such as faster construction, increased geometric complexity, waste minimisation, less human labour, improved accuracy and on-site safety improvements (Zhao & Loporcaro, 2019). Introducing this freeform method of construction into the concrete industry has the potential to create new innovative concrete shapes without formwork, and thus having a unique advantage over typical concrete construction.

Concrete additive manufacturing consists of the deposition of successive layers of concrete that is generally pumped to a nozzle whose size may vary in shape and dimensions (Bos et al., 2016). The nozzle can be attached to either a robotic arm, a frame or a gantry system and it is computer controlled. Cementitious materials used in additive manufacturing must possess characteristics different from those possessed by ordinary concrete. 3D printed concrete mix needs to have acceptable extrudability so it could be extruded through a small-size (e.g. 10 to 40 mm) nozzle. It must also have adequate open time to ensure adhesion between filament layers occurs and no cold joints are formed. The material must have sufficient buildability characteristics for the structure to be laid down correctly, remain self-supported and hold its shape under the increasing load generated by subsequent layers. The performance of the concrete is reliant on these characteristics, which are highly influenced by the workability of the material.

Although research on additive manufacturing of concrete is being conducted in many universities, research institutes and private companies, the technology is still in its infancy (Buswell et al., 2018). New Zealand is lagging behind. More research is required to develop solutions that account for the local requirements. In this paper, preliminary results are presented on the development of concrete mixes that will form the basis for further research currently being conducted at the University of Canterbury.

LITERATURE REVIEW

Printing technologies

Additive manufacturing has been employed in different industries (e.g. biomedical, aerospace, manufacturing, construction) over the last few decades. Almost any type of material can be 3D printed, from plastic to ceramics and from metals to concrete (Ngo et al., 2018). The origins of additive manufacturing are dated to the early 1980s when Charles Hull patented the stereolithography (SLA) process that used liquid photosensitive resins as printing materials (Hull, 2015). This process was soon followed by other 3D printing technologies such as material extrusion (MEX) binder jetting (BJT) , and Powder Bed Fusion (PBF). These technologies are well suited for polymers and metals. Also, they have provided the basis technologies for large scale 3D printing. For cementitious materials, other 3D printing processes have been developed. The most common are Contour Crafting (Khoshnevis, 2004), Concrete Printing (S. Lim, 2009), and D-shape (Dini). Due to the large scale of the 3D printing machines, the nozzle (the depositing head) is either mounted on a frame, a robot or a gantry. Contour crafting, patented by Prof. Behrokh Khoshnevis at the University of Southern California in 2004 was developed for in-situ applications. It comprises a gantry system, a pump and a nozzle. The concrete material is pumped to the nozzle from which the material is extruded, then the surface of the material printed is smoothed with a trowel (Khoshnevis, 2004). Concrete printing, developed by a research team from the University of Loughborough, employs a similar process based on concrete extrusion. This technology was conceived for off-site applications, however, in-situ applications are also possible. The concrete is pumped to a nozzle and then extruded. No trowelling system is employed. Concrete printing allows for greater control of the 3D printed geometries (Le et al., 2012). Similarly to Concrete Printing, the D-shape process was developed for off-site applications. It uses a powder deposition process where a binder is used to hardened selective layers of materials. Each layer of material is placed to the required thickness on the printing platform, then the nozzle deposits the binder only where the building material needs to be solidified. When the 3D object is completed, the loose material that has not hardened is removed. Examples of full-scale objects printed using the contour crafting, concrete printing and D-shape processes are shown in Figure 1.

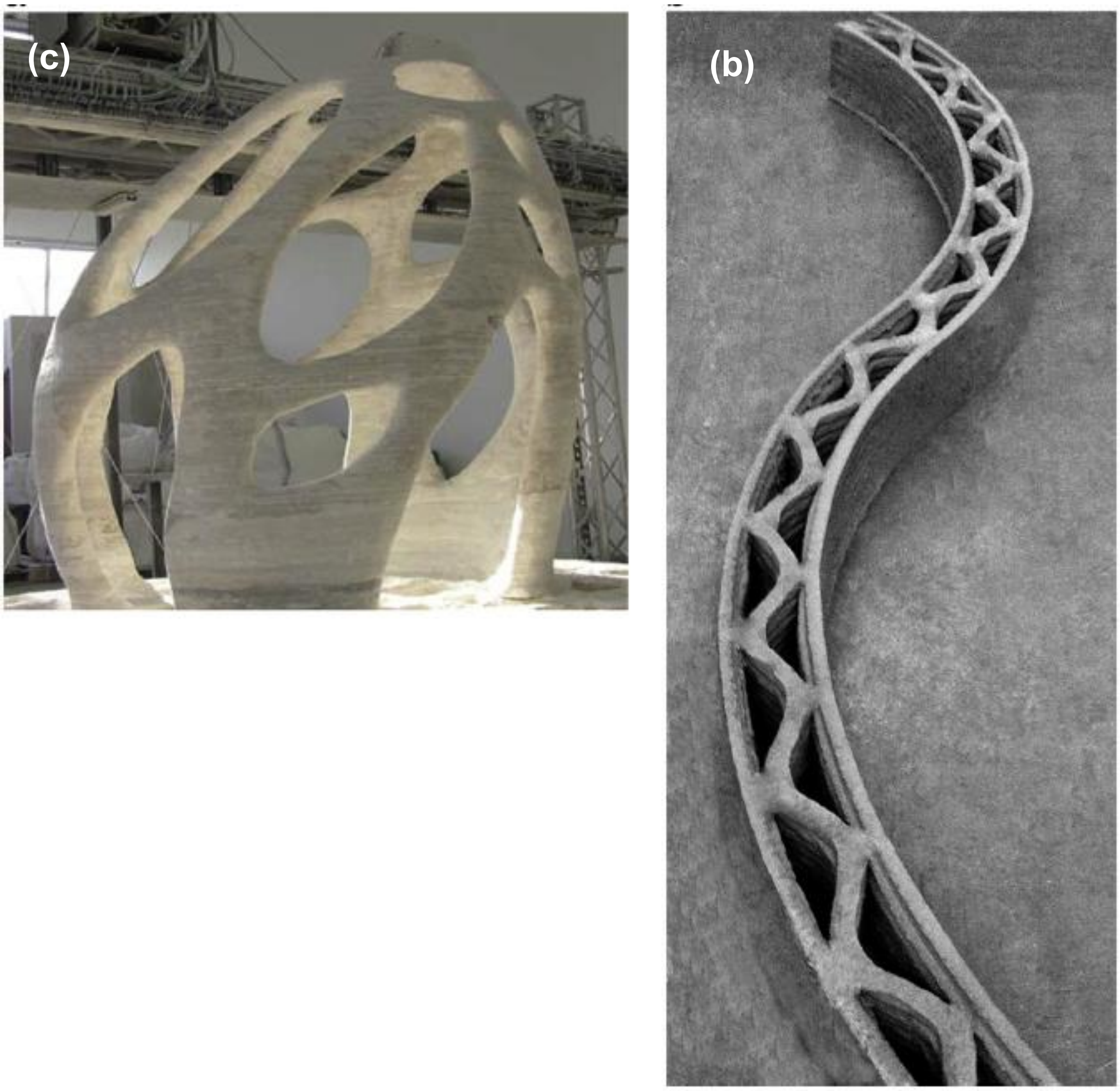

Figure 1 Examples of full-scale samples from Concrete Printing (a), Contour Crafting (b) and D-shape (c). Images are taken from Lim et al. (2012).

Concrete fresh properties and material mixes

Several concrete mixes have been developed by researchers involved in concrete additive manufacturing. The mixes are designed to suit the requirements of the 3D printer process adopted. Nevertheless, the fresh properties of concrete are the key to the success of 3D printing. The fresh properties that 3D concrete mixes must possess to be extruded by a nozzle are pumpability or workability, printability (or extrudability), open time, and buildability (Le et al., 2012; Lim et al., 2012).

Pumpability refers to the ease and reliability of pumping the concrete through the delivery system (from the pump to the nozzle). Printability or extrudability refers to the capacity of the material to be extruded through a nozzle as a continuous filament. The filament should have no or minimal deformation of cross-section as well as an acceptable level of splitting or tearing (Buswell et al., 2018). Buildability is the ability of the extruded layers of concrete to withstand the load applied by layers placed above without notable slumping. The printed concrete filaments must possess sufficient strength and stiffness to avoid significant deformation once further filaments are laid upon them. The open time is the time during which a concrete mix can be used in a 3D concrete printer. If the concrete is extruded beyond the open time, the mix may be too hard to be extruded. Also, the open time is associated with the hydration rate of the concrete mix. There must be sufficient adhesion between subsequent layers with no cold joints formed between them. The open time influences pumpability and extrusion. On the other hand, the open time is highly influenced by the mix viscosity, the yield strength (the minimum stress to initiate flow) and for how long the ideal value is maintained constant. The open time needs to be calibrated as a function of the volume of the printed object and its area (since this determines the total length of the deposited material per layer).

Concrete mix design developments have been carried out at Loughborough University by Le et al. (Le et al., 2012) using the concrete printing process. The 3D printer utilised was a prototype concrete machine supported by a 5.4 m (length) x 4.4 m (width) x 5.4 m (height) steel frame. The concrete material was fed from a container mounted on top of the printing head. A concrete pump was used to transport the mix from the container to the 9-mm printing nozzle. The printing head was digitally controlled in the X, Y and Z directions by a CNC machine. The optimum printable mix consisted of a 3:2 sand-binder ratio. The maximum size of the sand was 2 mm. This limit was governed by the size of the printing nozzle. The binder was made of cement CEM type I 52.5 (70%), fly ash (20%) and silica fume. A superplasticiser, a retarder and an accelerator were added to improve workability, to maintain a sufficient open time, and to control setting, respectively. Polypropylene fibres were used to reduce shrinkage and deformation in the plastic state (1.2 kg/m^2). The mix proportion of the optimum mix is summarised in Table 1. Paul et al. (Paul, 2018) investigated the fresh and the hardened properties of three types of mixes. The first mix was an alkali-activated geopolymer mortar with no cement. The second and third mixes were printable mortars made of sand (max size 1 mm), cement, fly ash, silica fume, plasticiser and water. The mix proportions of the cement-based mixes were the same. However, in mix 3, glass fibre was used to improve the flexural strength. In Table 1, only the proportion of mix 3 is presented (Paul, 2018). All three mixes were successfully printed with a robotic printer. The geopolymer mix was printed using a 10 mm x 20 mm rectangular nozzle, while the cement-based mortars were printed with an 8-mm diameter circular nozzle. It was found that to ensure better pumpability, the thixotropy of the 3D printed materials should be greater than 10000 [Nmm rpm], Also, the flexural and compressive strength of the printed samples were influenced by the shape of the nozzle orifice and the complexity of the printed objects. Kazemian et al. (Kazemian et al., 2017) investigated the fresh properties of 3D printing mixes studying the effects of nano-clay, silica fume, and fibres inclusions. ASTM C150 Type II Portland cement was used. Sand of 2.36 mm maximum size was used as aggregate. A polycarboxylate-based high-range water-reducing admixture (HRWRA) was used to reduce the amount of water and achieving the required flowability. Also, a viscosity modifying admixture (VMA) was added to increase plastic viscosity and cohesion. Polypropylene (PP) fibres 6-mm long were used to control shrinkage cracking. Silica fume was used as supplementary cementitious material to improve the cohesion of fresh concrete, the mechanical strength and the impermeability of the hardened concrete. In Table 1, two of the four mixes developed by Kazemian et al. are presented. The printer employed was a linear concrete printing machine capable to print up to ten layers of 1.2-m long filaments. The concrete was extruded through a 38.1 mm x 25.4 mm nozzle. It was found that small additions of nano-clay produced a noticeable increase in viscosity and cohesion. Trial-and-error experiments were carried out to determine the ideal mix proportions. A mix design was deemed successful when when the printed layers did not not have any surface defect; the layers edges were visible and squared (because a rectangular shape nozzle was used) and dimension conformity and consistency were satisfied. Dimension conformity guaranteed that the width of each layer was within 10% error from the target width (38.1 mm); meanwhile, dimension consistency required that any change in width of the single filament was less than 10% of the target width. The experimental results showed that additions of nano-clay and silica fume improved shape stability (buildability).

The mix designs discussed in this section and presented in Table 1 formed the basis of the mix developed in this research.

Table 1 Mix proportion of 3D printed concrete materials from selected literature

Material	**Mix proportion (kg/m^3)**			
	Le et al. (Le et al., 2012)	**Paul et al. (Paul, 2018)**	**Kazemian et al. (Kazemian et al., 2017)**	**Kazemian et al. (Kazemian et al., 2017)**
Sand	1241	1211	1357	1379
Cement	579	290	540	600
Fly ash	165	278		
Silica fume	83	145	60	
Fibres	1.2 (PP)	13.5 (glass)		1.18 (PP)
Water	232	284	259	259
Superplasticiser	1%[a]	7	0.16%[b]	0.06[b]
Retarder	0.5%[a]			
VMA				0.10[b]

[a] The percentages are reported by binder weight.
[b] The percentages are reported by cementitious materials mass.

Research aim and objectives

This research aims to develop and test the fresh properties of 3D concrete printing mixes from locally sourced materials and printed through a custom-design and built 3D concrete printer.

The following objectives have been identified:

- Develop three concrete mixes that can be extruded from the 10-mm nozzle available;
- Investigate and compare the fresh properties of the three mixes;
- Provide recommendations for future mix and machine development.

MATERIALS, METHODOLOGY AND TESTING

Mix design

A review of 3D printed concrete mixes available in the literature informed the design of three initial mixes (Table 1). Trial-and-error tests were performed to identify the proportion of the materials. The three selected mixes, named hereafter mix 1, 2 and 2, contained a different proportion of Portland Cement, aggregate (river sand, size smaller than 2.36 mm), fly ash, silica fume, water, a modified polycarboxylate-based superplasticiser, and polymer fibres.
The dry components (cement, sand, river sand, fly ash, silica fume) were added to a 5 L mortar mixer with water and a small amount of superplasticiser to reduce the water demand while increasing workability. Mix 1 was designed with no addition of fibres, mix 2 included polyvinyl alcohol (PVA) fibres and mix 3 polypropylene fibres. The three mixes required fine-tuning before being fully investigated. They had to be extruded through the nozzle with little or no deformation of the filament. Also, a 4-layer tall element could be built noticeable deformation of the bottom layer.

Custom-designed and built 3D concrete printer

In the additive manufacturing industry, there are many architectures of machine design for planar Material Extrusion (MEX) systems. Some use robotic arms with up to six degrees of freedom but for planar extrusion, only three are required, *x,y,* and *z*. Robotic arms are very effective, however, they are also very expensive, especially if a long reach and/or a heavy print head is required. A more cost-effective option is to use a Cartesian system controlling the x and y planar motion and z motion for the layer height. A scaled-down prototype machine has been manufactured and has been used in this research. The build volume is 1.5m x 2m x1.5m (*xyz*).

Where possible, industry-standard componentry was used. Low backlash ball screws on each axis provide an adequate reduction ratio to allow direct coupling of stepper motors. Similarly, a stepper motor is directly coupled to the screw extruder. The motor control system uses an Arduino microprocessor and standard electronic motor drives. Linear bearings are used for each slide. To avoid corrosion and the requirement to paint the structure, aluminium, stainless steel, and 3D printed polymer parts are used.

For ease of use and creating the G-Code for controlling the axes stepper motors, industry-standard Marlin firmware is used. The G-Code can be manually written using a text editor or, preferably, an industry-standard graphical user interface such as PrusaSlicer is used. This slicer is used on *xyz* polymer printers such as the low-cost Prusa MEX machines used by students at schools and universities. After customising the machine default settings, it is as simple as loading the component file and exporting the G-Code file for the printer. Specialist robotics know-how is not required to run the machine.

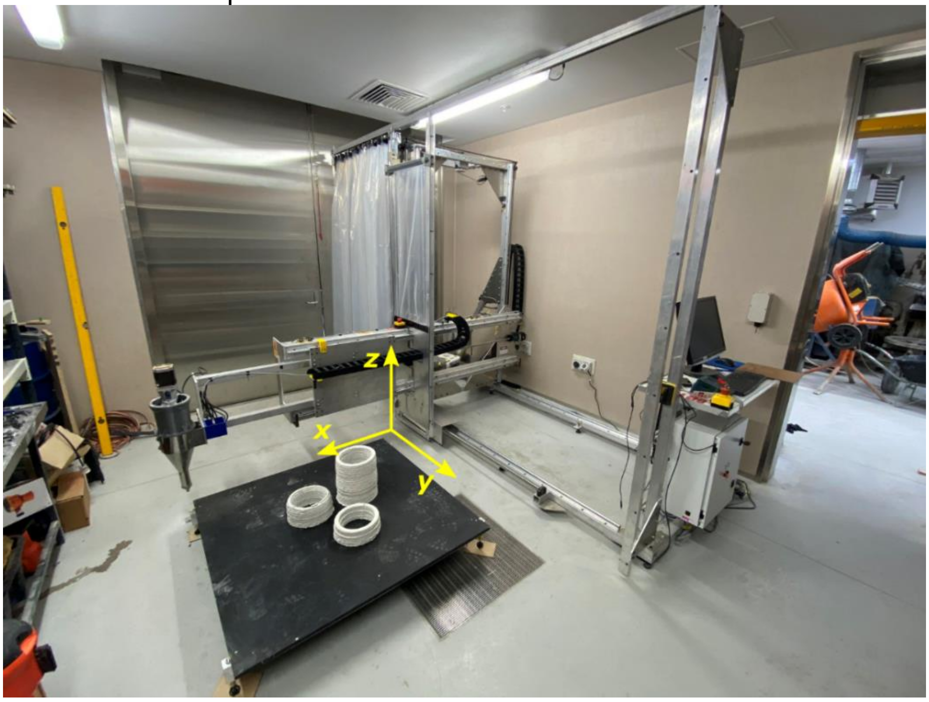

Figure 2 The UC custom-built 3D concrete printing machine.

Experimental testing: fresh properties

The fresh properties under investigation were: workability, extrudability, buildability and open time. Experimental tests were selected from a review of previous research and available standards. For each mix design, three samples were tested.

The custom-made printer was not provided with a pump, workability was tested instead of printability. For standard concrete, workability is evaluated using several conventional tests such as slump, compacting factor and flow tests (Kazemian et al., 2017; Le et al., 2012). In this research, the workability of the mixes was quickly assessed using the ASTM drop table test following the ASTM C1437-20 standard (International, 2020). The test requires placing the freshly mixed concrete into a mould, tamping it 20 times with a tamper to ensure uniform filling of the mould, then dropping the table 25 times in 15 seconds. The spread in four directions is then measured using a Vernier calliper and averaged for three different mix designs.

Extrudability was tested using a filament test proposed by Le et al. (Le et al., 2012). This involved printing a U-shape filament with the longest sides being 300 mm long, while the shortest side was 40 mm. This configuration allowed to test the concrete extrudability and the corner section properties. The lines were extruded with a 9 mm clearance from the printer build platform board at a linear speed of 2,000 mm/min. Filaments were scored on a scale between 1 and 5, with 5 being the lines perfectly extruded and consistent without any significant deformation, tearing or splitting and 1 if the concrete did not extrude at all. This test ensured the mix came out consistently without any significant deformation.

Buildability was measured by extruding four layers of concrete one on top of the other. A two-minute setting time in between each layer was allowed for the concrete to partially set. The width of the top and bottom layers was measured using a Vernier calliper approximately 24 hours after the extrusion. Measurements were taken at three different locations for each layer. The three results were averaged. A percentage difference was taken between the top and bottom layer widths.
Two separate methods were adopted to determine the open time. The first method consisted in measuring the change in shear strength with time using a shear vane apparatus (Le et al., 2012). Austin et al. (Austin et al., 2005) adopted the shear vane test typically used to measure the shear strength of soil to determine concrete workability. The concrete mixes under investigation were placed into a rectangular base 100 mm x 100 mm x 50 mm deep container, the shear strength was recorded at set intervals of 0 (for workability), 5, 15, 30, 60, 90 and 120 minutes using a 19-mm diameter shear vane apparatus. The shear vane had a height of 29mm, which was inserted into the concrete samples, as shown in Figure 3.

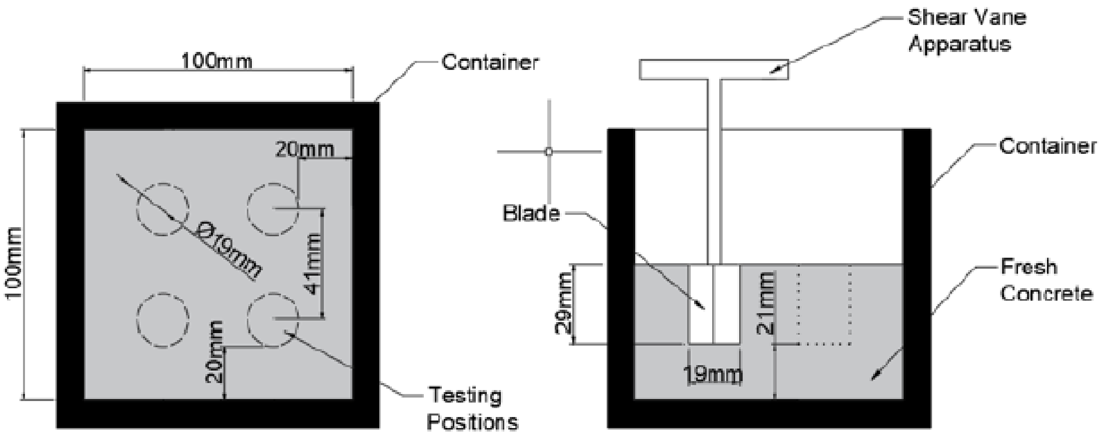

Figure 3 Diagram of the shear vane used for the open time testing

The second test method to evaluate the open time consisted in visually inspecting 3D printed samples for imperfections such as cold joints (Buswell et al., 2018; Jo et al., 2020). Cross-section tests were taken on all the samples printed using the three mix designs. The four-filament tall samples used for buildability were let to set for approximately 24 hours, then cut through. This enabled the inspection of air bubbles, cold joints and other imperfections. The condition of the cross-section of the sample was scored on a scale from 1 to 5, with 1 being a section with major imperfections (e.g. air bubbles and cold joints), and 5 being a section with no imperfections.

RESULTS AND DISCUSSION

Mix design

The tested mix designs are presented in Table 2. These mix designs were all printable using the UC custom-made 3D printer and could be replicated when the volume of the mix was increased. The total density of the three mixes varied between 2260 kg/m^3 and 2311 kg/m^3.

Table 2. Proportions of the tested mix designs.

Materials	**Mix proportion [kg/m^3]**		
	Mix 1	**Mix 2**	**Mix 3**
Sand	1140	1229	1334
Cement	644	571	503
Fly ash	188	163	144
Silica fume	94	82	72
Water	241	217	202
Fibres	0	1.2 (PVA)	1.2 (Polypropelene)
Superplasticiser	4	4.3	4.6
Total	2311	2267	2260
W/C ratio	0.26	0.27	0.28
Binder to sand ratio	0.81	0.66	0.54

As aggregate river sand was used,sieve analysis was performed on the sand to determine the particle size distribution (Figure 4). The aggregate is relatively well-graded. Using a better-graded aggregate would increase the density of the mix design and in turn, increase the ultimate strength of the concrete. If required, the density can also be increased through proper vibration of the sample to reduce entrapped air and using a suitable curing system to prevent water evaporation and decrease porosity.

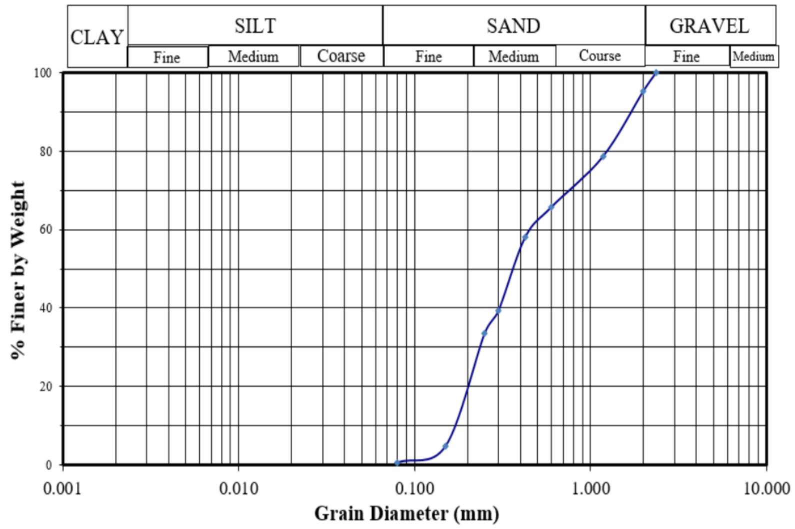

Figure 4. Particle distribution curve for river sand.

Workability

The drop table test was performed three times for each mix design. The results were then averaged. They are summarised in Table 3. The variability of the results from the drop table test among the mixes is largely due to the presence and type of reinforcement fibres used.

The role of the fibres is to reduce plastic shrinkage and deformation at the fresh state. Mix design 1, with the largest spread, has no reinforcement. The workability is lower in mix three with the polypropylene fibres than that of the mix with PVA fibres due to the nature of the polypropylene fibres. PVA fibres ($E \approx$ 30-40 GPa) are stiffer than polypropylene fibres ($E \approx$ 3.5 GPa). This means they are less inclined to mould and bond with the surrounding particles. The polypropylene fibres are very flexible and will combine throughout the mix to provide tensile resistance and hold the shape most effectively.

Table 3. ASTM drop table test average spread results

	Mix 1	Mix 2	Mix 3
Average lateral spread [mm]	193.42	180.63	171.33

Extrudability

The extrudability test was performed on each of the mixes twice. The maximum and minimum width and depth of each of the extruded filaments were measured. The results are presented in Table 4. The results show that the mix with the polypropylene fibres (mix 3) extruded a narrower and less consistent filament, with the width varying by over 7 mm in trial two. The widths of the filament extruded with Mix 1 and 2 were similar (~23mm). Moreover, they were more consistent in both width and depth in the two tests. Figure 5 shows the extruded single and double filament from the first test of the mix with the PVA fibres (mix 2).

Table 4 Extrudability test results: max and min-width and depth of a single layer filament

	Mix 1	Mix 2	Mix 3
Max width [mm]	24.180	24.080	18.745
Min width [mm]	22.480	22.095	11.635
Max depth [mm]	10.005	10.415	9.000
Min depth [mm]	9.230	10.065	7.145

Figure 5 Mix 2 with PVA extrudability test trial one.

It must be noted that after 24 hours, shrinkage cracks were noticed on the filaments of mix 1, most likely caused by the lack of fibre reinforcement. A subjective “extrudability score” was assigned on both trials of the three mixes. The scores are summarised in Table 5

Table 5 Extrudability scores for mix 1, 2 and 3 and trial 1 and 2

	Score	Total
Mix 1, Trial 1	5	9.5
Mix 1, Trial 2	4.5	
Mix 2, Trial 1	4	9
Mix 2, Trial 2	5	
Mix 3, Trial 1	2.5	5.5
Mix 3, Trial 2	3	

Open time

The open time was determined by measuring the increase in shear strength (τ) with time (t) using the shear vane apparatus. Shear strength was measured at 0, 5, 15, 30, 60, 90 and 120 minutes. Each data point in Figure 6 represents the average of three measurements. A linear regression analysis was performed to fit the testing results.

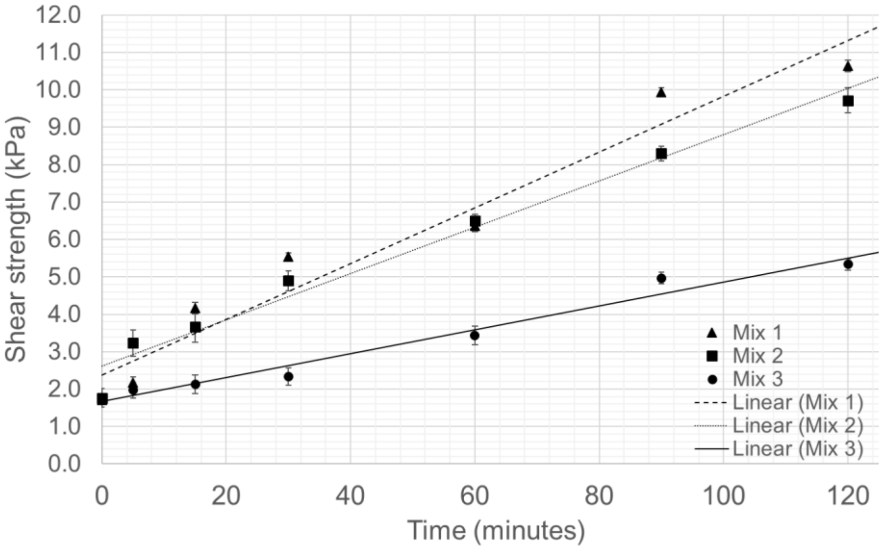

Figure 6 Shear vane test results for workability: shear strength versus time

The linear regressions derived from the shear strength versus time data are represented by the following equations:

Mix 1	$\tau = 0.0745\ t + 2.3814$	$R^2 = 0.952$
Mix 2	$\tau = 0.0618\ t + 2.6145$	$R^2 = 0.976$
Mix 3	$\tau = 0.032\ t + 1.6664$	$R^2 = 0.974$

The initial shear strength (at t = 0) of the concrete mixes was approximately similar ranging between 1.5 and 2 kPa. However, the rate of shear strength increase varied. The increase in shear strength of mix 3 was significantly slower compared to mix 1 and 2. Therefore, mix 3 was much slower to gain shear strength. Accelerated hydration of concrete may result in a shorter open time and possibly cold joints at the interface between layers. It was observed that once the shear strength of the concrete increased by 1 kPa, the mixture became difficult to be extruded. Therefore, it was established that the open time was the time required for the mix to gain 1 kPa shear strength. Based on this criterion and using the linear regression equations derived from the shear strength versus time data, the calculated open times are: 13’ 42” for mix 1, 16’ 18” for mix 2 and 31’ 25” for mix 3.

A visual inspection of the cross-section of the concrete filament was performed to observed any cold joint. Inspections were performed 24 hours after printing 500-mm long and 4-layer tall filaments. It must be noted that a 2-minute pause was allowed between the printing of each layer. The visual inspection (see Figure 7) showed that no cold joints had formed between layers for any of the samples. There was also no notable air bubbles or other imperfections.

Figure 7 Visual inspection of the filament cross-section (Mix 1 on the left, Mix 2 on the centre and Mix 3 on the right image)

Buildability

Buildability was assessed as the ability of the concrete filament to hold its structure without significant deformation (lateral spread) once layers were added on the top. The 4-layer tall filament samples used for the open time test were used (see Figure 7). For each mix, the width of the top and bottom layers were measured. Then, the percentage change of the bottom layer width compared to the top filament width are presented in Figure 7.

Table 6 Buildability test results

	Mix 1	**Mix 2**	**Mix 3**
Botton layer width [mm]	34.18	27.375	22.80
Top layer width [mm]	17.32	26.51	17.87
Percentage change in width	97.3 %	3.3%	27.6%

Mix 1 which did not contain fibres underwent the largest deformation under the load produced by the top layers. The increase in width was 97.3%. Mix 1 had difficulties with withstanding the load from the top layers due to the lack of fibre reinforcement. Mix 2 and 3, which contained fibres performed better with a 3.3% and 27.6% increase in the bottom layer width, respectively. Mix 2, containing the PVA fibres, performed the best by maintaining a constant width. This may be attributed to the lowest water-cement ratio and superplasticiser content.

CONCLUSIONS

Concrete additive manufacturing is a promising technology. It has the potential to revolutionise the concrete construction industry due to its ability to manufacture architectural and structural components without the constraints of formwork, the opportunity to automate the design and construction phases, increase concrete placement accuracy, improve workers' health and safety, etc.

High performance 3D printable concrete mixes were developed. Fresh properties such as extrudability, buildability, open time and workability were investigated. The results showed that mix 2 was best suited for 3D printing and further research is required for further improvements. The mix had a 3:2 sand-binder and 0.27 water-cement ratio. The binder was approximately 70% cement, 20% fly ash and 10% silica fume. PVA fibres in the quantity of 1.2 kg/m^3 were added to the mix to avoid plastic shrinkage. The mix showed the best workability and extrudability through a 10 mm printer nozzle. It also showed little deformation under loading caused the subsequent top layers. 3D concrete.

ACKNOWLEDGEMENTS

The authors would like to acknowledge the Civil Engineering students Jake Potton, Richard, for performing the testing; Mechanical Engineering students Mink Witowski and Talyah Mayron who assisted with the design of the 3D concrete printing machine; Tim Perigo, Julian Phillips, Mechanical Engineering staff, for building the machine and Associate Professor Allan Scott for sharing his knowledge.

REFERENCES

Austin, S. A., Goodier, C. I., & Robins, P. J. (2005, 2005/03/01). Low-volume wet-process sprayed concrete: pumping and spraying. *Materials and Structures, 38*(2), 229. https://doi.org/10.1007/BF02479348

Bos, F., Wolfs, R., Ahmed, Z., & Salet, T. (2016, 2016/07/02). Additive manufacturing of concrete in construction: potentials and challenges of 3D concrete printing. *Virtual and Physical Prototyping, 11*(3), 209-225. https://doi.org/10.1080/17452759.2016.1209867

Buswell, R. A., Leal de Silva, W. R., Jones, S. Z., & Dirrenberger, J. (2018, 2018/10/01/). 3D printing using concrete extrusion: A roadmap for research. *Cement and Concrete Research, 112*, 37-49. https://doi.org/https://doi.org/10.1016/j.cemconres.2018.05.006

Dini, E. *D-shape*. https://d-shape.com/

Hull, C. W. (2015). The birth of 3D printing. *Research-Technology Management, 58*(6), 25-30.

International, A. (2020). *C1437-20*. West Conshohocken, PA 19428-2959. United States.

Jo, J. H., Jo, B. W., Cho, W., & Kim, J.-H. (2020, 2020/03/03). Development of a 3D Printer for Concrete Structures: Laboratory Testing of Cementitious Materials. *International Journal of Concrete Structures and Materials, 14*(1), 13. https://doi.org/10.1186/s40069-019-0388-2

Kazemian, A., Yuan, X., Cochran, E., & Khoshnevis, B. (2017, 2017/08/01/). Cementitious materials for construction-scale 3D printing: Laboratory testing of fresh printing mixture. *Construction and Building Materials, 145*, 639-647. https://doi.org/https://doi.org/10.1016/j.conbuildmat.2017.04.015

Khoshnevis, B. (2004, 2004/01/01/). Automated construction by contour crafting—related robotics and information technologies. *Automation in Construction, 13*(1), 5-19. https://doi.org/https://doi.org/10.1016/j.autcon.2003.08.012

Le, T. T., Austin, S. A., Lim, S., Buswell, R. A., Gibb, A. G. F., & Thorpe, T. (2012, 2012/08/01). Mix design and fresh properties for high-performance printing concrete. *Materials and Structures, 45*(8), 1221-1232. https://doi.org/10.1617/s11527-012-9828-z

Lim, S., Buswell, R. A., Le, T. T., Austin, S. A., Gibb, A. G. F., & Thorpe, T. (2012, 2012/01/01/). Developments in construction-scale additive manufacturing processes. *Automation in Construction, 21*, 262-268. https://doi.org/https://doi.org/10.1016/j.autcon.2011.06.010

Ngo, T. D., Kashani, A., Imbalzano, G., Nguyen, K. T. Q., & Hui, D. (2018, 2018/06/15/). Additive manufacturing (3D printing): A review of materials, methods, applications and challenges. *Composites Part B: Engineering, 143*, 172-196. https://doi.org/https://doi.org/10.1016/j.compositesb.2018.02.012

Paul, S. C., Tay, Y. W. D., Panda, B., & Tan, M. J. (2018). Fresh and hardened properties of 3D printable cementitious materials for building and construction. *Archives of civil and mechanical engineering, 18*, 1-8.

S. Lim, T. L., J. Webster, R. Buswell, S. Austin, A. Gibb, T. Thorpe. (2009). *Fabricating construction components using layer manufacturing technology* Global Innovation in Construction Conference, Loughborough University, Leicestershire, UK.

Soderstrom, M. (2020). *Concrete : From Ancient Origins to a Problematic Future*. University of Regina. http://ebookcentral.proquest.com/lib/canterbury/detail.action?docID=6362824

Zhao, A., & Loporcaro, G. (2019, October 2019). *Exploring opportunities and limitations of 3D concrete printing technology in New Zealand* Concrete NZ conference, Dunedin.